Neurobiology of Aging 36 (2015) 2164–2175

Contents lists available at ScienceDirect

Neurobiology of Aging

journal homepage: www.elsevier.com/locate/neuaging

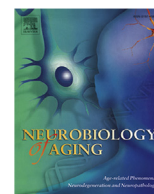

Telomere dysfunction reduces microglial numbers without fully inducing an aging phenotype

Asif Manzoor Khan [a], Alicia A. Babcock [a], Hamid Saeed [b], Christa Løth Myhre [a], Moustapha Kassem [b], Bente Finsen [a,*]

[a] Department of Neurobiology Research, Institute of Molecular Medicine, University of Southern Denmark, Odense C, Denmark
[b] Department of Endocrinology and Metabolism, Odense University Hospital, University of Southern Denmark, Odense C, Denmark

ARTICLE INFO

Article history:
Received 15 July 2014
Received in revised form 3 March 2015
Accepted 10 March 2015
Available online 14 March 2015

Keywords:
Dentate gyrus
Replicative senescence
Spatial learning
Cellular apoptosis
Optical fractionator
Global spatial sampling

ABSTRACT

The susceptibility of the aging brain to neurodegenerative disease may in part be attributed to cellular aging of the microglial cells that survey it. We investigated the effect of cellular aging induced by telomere shortening on microglia by the use of mice lacking the telomerase RNA component (TERC) and design-based stereology. TERC knockout (KO) mice had a significantly reduced number of CD11b$^+$ microglia in the dentate gyrus. Because of an even greater reduction in dentate gyrus volume, microglial density was, however, increased. Microglia in TERC KO mice maintained a homogenous distribution and normal expression of CD45 and CD68 and the aging marker, ferritin, but were morphologically distinct from microglia in both adult and old wild-type mice. TERC KO mice also showed increased cellular apoptosis and impaired spatial learning. Our results suggest that individual microglia are relatively resistant to telomerase deficiency during steady state conditions, despite an overall reduction in microglial numbers. Furthermore, telomerase deficiency and aging may provide disparate cues leading to distinct changes in microglial morphology and phenotype.

© 2015 Elsevier Inc. All rights reserved.

1. Introduction

Microglial cells are myeloid-lineage cells that form the first line of immune defense of the central nervous system (CNS) (Hanisch and Kettenmann, 2007; Ransohoff and Perry, 2009). Microglia originate from primitive myeloid progenitors in the embryonic yolk sac, which populate the CNS during prenatal development (Alliot et al., 1999; Ginhoux et al., 2010; Kierdorf et al., 2013) and then expand by proliferation to reach the high microglial numbers present in the adult CNS (Dalmau et al., 2003). A low baseline proliferation (Babcock et al., 2013; Lawson et al., 1992; Wirenfeldt et al., 2007) and scattered progenitor cells (Elmore et al., 2014) are available to maintain the microglial population. Microglia respond to acute tissue injury, such as axonal and ischemic injury, by altering their morphology and gene expression and by undergoing increased cell division (Ladeby et al., 2005a; Lehrmann et al., 1997; Wirenfeldt et al., 2007). In vivo 2-photon laser-scanning microscopy showed that the distal branches of "resting", ramified microglia have highly motile fine protrusions, allowing microglial cells to continually survey the cellular environment (Davalos et al., 2005; Nimmerjahn et al., 2005). Dead cells or cellular debris are thereby rapidly taken up and cleared from the neuropil by surveying microglia (Babcock et al., 2015; El Khoury et al., 1996; Hickman et al., 2008; Nielsen et al., 2009).

Microglia alter their morphology and surveillance capacity with advanced aging (Baron et al., 2014; Hefendehl et al., 2014), which is a major risk factor for neurodegenerative diseases, such as Alzheimer's and Parkinson's disease (Raivich et al., 1999; Streit et al., 1999; Wong, 2013). Aging is characterized by increased cellular senescence, due to accumulation of DNA damage and shortening of telomeres (Blackburn et al., 2006; Blasco, 2007a). Highly proliferative cells like stem cells, germ line cells, and cancer cells have increased telomerase activity to maintain telomere length (Finkel et al., 2007; Satyanarayana et al., 2004; Shay and Wright, 2005). In comparison, replication is limited in somatic cells, which have less telomerase activity and shorter telomeres (Blasco, 2007a; Blasco et al., 1997; Finkel et al., 2007). Thus, healthy somatic cells eventually become dysfunctional and become senescent (Blasco, 2007a; Collado et al., 2007). Mice lacking the telomerase RNA component (TERC) (TERC knockout [KO] mice) display an accelerated-aging phenotype after successive generations of mating, which results in shortened telomeres (Blasco et al., 1997; Saeed et al., 2011).

Telomere shortening has been suggested to render microglia susceptible to age-associated dystrophy and make the brain prone

* Corresponding author at: Neurobiology Research, Institute of Molecular Medicine, University of Southern Denmark, J.B. Winsloewsvej 25-2, DK-5000 Odense C, Denmark. Tel.: +45 6550 3990; fax: +45 6550 3950.
E-mail address: bfinsen@health.sdu.dk (B. Finsen).

0197-4580/$ – see front matter © 2015 Elsevier Inc. All rights reserved.
http://dx.doi.org/10.1016/j.neurobiolaging.2015.03.008

to neurodegenerative disease (Streit, 2006; Streit et al., 2009; Wong, 2013). Reduced telomerase activity and telomere shortening were found in microglia from aging rats and humans (Flanary and Streit, 2004; Flanary et al., 2007). To the contrary, however, inducing telomere dysfunction by TERC deficiency in a transgenic mouse model of Alzheimer's disease reduced amyloid pathology and improved spatial learning (Rolyan et al., 2011). Based on the demonstration of increased microglial density and reduced process length and process branching of individual microglial cells in TERC KO mice, Rolyan et al. (2011) suggested that telomere dysfunction induced microglial activation. However, they observed no evidence of increased microglial proliferation or increased expression of inflammatory markers (Rolyan et al., 2011).

To improve our understanding of the consequences of telomere dysfunction on microglia during aging, we have combined the use of immunohistochemistry and design-based stereology (West et al., 1996; Wirenfeldt et al., 2003) to study microglial numbers, morphology, and phenotype in the dentate gyrus of telomerase-deficient TERC KO mice. Because gender and age (in female mice) were previously reported to impact microglial numbers in the murine dentate gyrus (Mouton et al., 2002), mice of both genders and of different ages were included. Our results demonstrate that the increased microglial density previously reported in TERC KO mice (Rolyan et al., 2011) in reality reflects a reduction in the number of microglia, which is superseded by an even greater reduction in dentate gyrus volume. These findings apply to mice of both genders, which we find have comparable numbers of microglia at all ages investigated. Importantly, our results reveal distinct differences in the morphology and phenotype of microglia in TERC KO mice compared with microglia in both adult and old wild-type (WT) mice suggesting that telomerase deficiency and aging provide disparate cues to microglia. These findings carry implications for improving the understanding of the molecular interaction between neurons and microglia during healthy and pathological aging.

2. Materials and methods

2.1. Experimental material

2.1.1. Mouse breeding, genotyping, and handling

Mice carrying a homozygous germ-line deletion for the *Terc* gene were used. TERC KO mice (Jackson Laboratories, strain 004132) are deficient in TERC, leading to complete knockdown of TERC expression and telomerase activity. TERC KO mice were maintained on a C57BL/6J background and were intercrossed to generate third generation TERC KO (G3 KO) mice. A few second-generation TERC KO (G2 KO) mice were also included in the study. Genotyping was done using the protocol provided by Jackson Laboratories. Age-matched and old C57BL/6J mice were used as WT controls. The mice were housed under a constant light and/or dark cycle with free access to standard chow and water. A total of 120 mice were used in the study. Protocols were approved by the Danish ethical animal care committee (permissions no. 2011/562–67 and 2011/561–1950).

2.1.2. Perfusion and tissue processing

The mice were deeply anesthetized by pentobarbital overdose (200 mg/mL) (Glostrup Apotek, Denmark) and perfused with 10 mL of 0.15 M Sørensen's phosphate buffer (pH 7.4) followed by 20 mL of 4% paraformaldehyde (PFA) in Sørensen's phosphate buffer. The brains were post-fixed in 4% PFA overnight and then 1% PFA for 24 hours at 4 °C. The brains were cut into 60-μm thick horizontal sections on a vibratome (Leica, VT1000 S). The free-floating sections were sampled in 4 parallel series and stored in a cryoprotective solution at −20 °C, as previously described (Wirenfeldt et al., 2003).

2.2. Histology

2.2.1. Primary antibodies and control antibodies

Rat monoclonal anti-mouse CD11b (Clone 5C6; Serotec, UK), rat monoclonal anti-mouse CD45 (Clone IBL-3/16; Serotec), rabbit polyclonal anti-Iba1 (Wako, Germany), rabbit polyclonal anti-cleaved poly (ADP ribose) polymerase (cPARP) (Abcam, UK), biotinylated rat monoclonal anti-mouse CD68 (Clone FA-11; Serotec), and rabbit polyclonal anti-human ferritin (Sigma-Aldrich, USA) were used. Rat IgG2b (RTK4530; Abcam), rat IgG1 (RTK2071; BioLegend, USA), and rabbit IgG (X0903; Dako, Denmark) were used for controls.

2.2.2. Diaminobenzidine immunohistochemistry

Single immunohistochemical stainings were performed using established methods for staining of thick free-floating sections using chromogenic development with diaminobenzidine (DAB) (Wirenfeldt et al., 2003). Nonspecific binding of primary antibodies was blocked by immersing sections in Tris-buffered saline (TBS) containing 10% fetal calf serum (FCS) for 1 hour at room temperature (RT). Incubation with the primary antibodies diluted in TBS containing 10% FCS took place for 1 hour at RT, followed by 1–2 days at 4 °C. Endogenous peroxidase activity was blocked by immersing sections in TBS with 10% methanol containing 3% H_2O_2 for 10 minutes. Incubation with the secondary reagents, which included biotinylated goat anti-rat and anti-rabbit antibodies (GE Healthcare, UK), as well as anti-rabbit EnVision + horse radish peroxidase (HRP)-labeled polymer (Dako), which were diluted in TBS containing 10% FCS and 1% Triton-X, took place for 1 hour at RT. Sections stained with biotinylated antibodies were incubated in streptavidin-conjugated HRP (Dako) diluted in TBS containing 10% FCS for 1 hour at RT. All sections were developed with 0.05% DAB in TBS containing 0.01% H_2O_2. Sections were finally mounted on gelatinized slides, air-dried, dehydrated in graded ethanol, cleared in xylene, and coverslipped with Depex mounting medium. The CD11b-stained sections used for stereological estimation of microglial cell numbers were counterstained with toluidine blue before dehydration and mounting. The sections used for stereological estimation of microglial process length, number of nodes, and cell body volume were incubated with rabbit–anti-mouse Iba1-antibody followed by anti-rabbit EnVision$^+$ HRP-labeled polymer, then developed with DAB, as described previously. To preserve the morphological details, these sections were not counterstained with toluidine blue.

2.2.3. Alkaline phosphatase immunohistochemistry

For visualization of cPARP for cellular quantification, sections were incubated with 10% FCS in TBS for 30 minutes followed by incubation overnight at 4 °C with polyclonal rabbit anti-cPARP antibody diluted 1:100 in TBS containing 10% FCS. The sections were rinsed 3 × 15 minutes in TBS + 1% Triton and then incubated with alkaline phosphatase (AP)-conjugated goat anti-rabbit IgG (Sigma-Aldrich, USA) diluted 1:200 in TBS containing 10% FCS, for 1 hour at RT. Sections were rinsed 3 × 15 minutes in TBS, followed by 15 minutes rinse in 10 mM Tris-HCl buffer, and development in a Tris-HCl-$MgCl_2$ buffer, containing nitro-blue tetrazolium chloride and 5-bromo-4-chloro-3-indolylphosphate p-toluidine salt and levamisole to block endogenous AP activity. Sections were mounted and coverslipped with Aquatex (Merck, Germany).

2.2.4. Double immunohistochemistry for cPARP and CD11b

CD11b staining was first developed using DAB, and then the sections were stained for cPARP using the AP method combined with a Vector Red Substrate kit (Vector Laboratories, Burlingame,

Download English Version:

https://daneshyari.com/en/article/6804271

Download Persian Version:

https://daneshyari.com/article/6804271

Daneshyari.com